Proceedings of the IASS 2024 Symposium
Redefining the Art of Structural Design
August 26-30, 2024, Zurich Switzerland
Philippe Block, Giulia Boller, Catherine DeWolf,
Jacqueline Pauli, Walter Kaufmann (eds.)

Study on mechanical properties of a 35-meter-span three-dimensional cable-truss flexible photovoltaic support system

Yunqiang Wu*, Yue Wu, Xiaoying Sun

* School of Civil Engineering, Harbin Institute of Technology, Harbin 150090, China.
qfmz_wyq@163.com.

Abstract

The flexible photovoltaic support system is one of the systems that have been proposed to support photovoltaic modules with wide application potential in recent years. It has the advantages of large span, fast construction speed, and can adapt to complex environments. This kind of support system can be used in large-span and complex scenes such as sewage treatment plants, fish ponds, mountains, and farms. However, this type of support system still has some problems, such as low stiffness, limited span, and insufficient wind resistance. To improve the span and stiffness and widen the application scene of the flexible photovoltaic support system, a new type of three-dimensional cable-truss flexible photovoltaic support system is proposed in this study. In this study, the finite element model of the new system is established first, and the accuracy of the finite element simulation is verified by the full-scale model test. Then, the advantages of the three-dimensional cable-truss flexible photovoltaic support system are illustrated from the aspects of natural frequency, mode, and mechanical properties through the finite element model. Finally, to better understand the mechanical characteristics of the system, parametric analysis is carried out. The results show that the finite element model can accurately simulate the stress state of the flexible photovoltaic system, and the new flexible photovoltaic support system has a good bearing capacity and structural stiffness and has a wide application prospect in large-span scenes such as wastewater treatment plants and fish ponds.

Keywords: Flexible photovoltaic support system, Finite element simulation, Mechanical properties, parameterization.

1. Introduction

Photovoltaic power generation technology is more and more widely used in the world. As a kind of photovoltaic module support system, the flexible photovoltaic support system has been widely studied and applied in recent years because of its advantages such as large span, good economy, and wide terrain. In 2008, Baumgartner et al. first proposed the single-layer cable support flexible photovoltaic system, known as "Solar Wings.", and then designed some new flexible photovoltaic systems for parking lots and ski resorts [1-5]. Later, Tamura, Kim, Ma Wenyong, Wang Zeguo, et al. studied the wind resistance of the single-layer cable support flexible photovoltaic support system and concluded that the wind resistance of the system was weak and wind-induced vibration was obvious [6-10]. To improve the span of flexible photovoltaic support systems, double-layer cable-supported flexible photovoltaic systems have gradually been widely concerned and applied recently [11-17]. However, if no wind suppression measures are taken, the double-layer cable-supported flexible photovoltaic system also has insufficient stiffness and obvious wind-induced vibration problems when used in strong wind conditions. The study of He and Chen et al. showed that the critical wind speed of the double-layer cable-supported flexible photovoltaic support system without wind suppression measures was only about 18.5m/s in a uniform wind field, and effective wind suppression measures were proposed [11-13, 18,19].

The above research shows that the existing flexible photovoltaic support system has some shortcomings, such as poor stiffness and insufficient wind resistance, which also limits its use. To improve the stiffness of the photovoltaic system, a new three-dimensional cable-truss flexible photovoltaic support system with better stiffness is proposed. In this study, the finite element model of the flexible photovoltaic system is established, and a full-scale model is used to verify the accuracy of the simulation results. Then the advantages of the new system in frequency, mode, and mechanical properties are demonstrated by the finite element model. Finally, the mechanical properties of the new system are studied in detail by parametric analysis. The research results are of great significance to the application of flexible photovoltaic support systems.

2. Proposal of the new structure

2.1 Introduction of the new system

This new system is composed of component cable(cable 1 and cable 2), stability cable(cable 3), triangle connection system, vertical support system and PV module (figure. 1). The unbalanced force of the vertical support system is balanced by the stay cable. Component cable and stability cable are arranged along the X direction, the initial deflection-span ratio of the component cable is 1/25, and the initial rise-span ratio of the stability cable is 1/15. Five groups of triangular connection systems are arranged at 1/6, 2/6, 3/6, 4/6, and 5/6 along the X direction. The triangle connection system is composed of cable 5, cable 6, and a compression rod. The PV module can be directly installed on the component cable, and the tilt angle of the PV module can be 0°-30°. The system can change the structure span, the initial tension, and the tilt angle of the PV module according to site conditions.

The initial tension of the component cable is 45kN and the initial tension of the stability cable is 55kN. The component cable and stay cable are galvanized stranded wire with diameters of Φ15.2. The stability cable adopts galvanized stranded wire with diameters of Φ12.7. The tensile strength of galvanized stranded wire is 1860MPa. The vertical support system is made of steel with a yield strength of 355MPa. The PV modules are connected directly to the component cable and tilted at 20 degrees. The PV module type is 2256mmx1133mmx35mmx545W, and a single module weighs 32.5kg. The material characteristics are shown in Table 1. The commercial nonlinear finite element software 3D3S was used to analyze the nonlinear mechanical properties of the three-dimensional cable-truss flexible photovoltaic support system (figure. 3). In the finite element model, we do not consider the role of the stay cable, and set the column to be fixed. The 35-meter span full-scale test was carried out in Wuhu City, Anhui Province, China, as shown in the figure. 1.

Table 1: Material properties

Name	type（mm）	Strength（MPa）	Density（kg/m3）	Elasticity modulus (Pa)	Poisson's ratio
Vertical support system	--	355	7850	2.06x1011	0.3
Compression rod	Φ32*2.5	355	7850	2.06x1011	0.3
Cable 5(cable 6)	Φ8	1770	11500	1.90x1011	0.3
Component cable and stay cable	Φ12.7	1860	8100	1.85x1011	0.3
Stability cable	Φ15.2	1860	8100	1.69x1011	0.3
PV module	2256mmx1133mm x35mmx545W	--	1927	5.5x1010	0.2

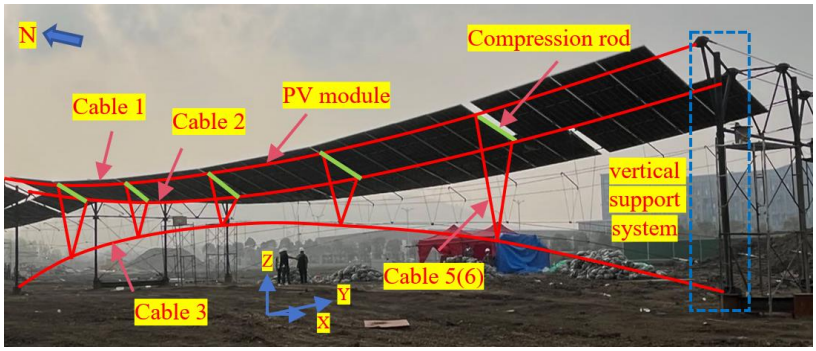

Figure. 1. Prototype drawing of full-scale test model.

2.2 Model accuracy verification

The tensile installation and static loading are tested by the full-scale test. The full-scale model shows that when the initial prestress of cable components is 45kN and the initial tension of stability cable is 25kN and 55kN respectively, the first-order frequencies of the system are 1.45Hz and 1.75Hz respectively. The mechanical properties of the system were studied by finite element software. The results show that when the initial tension of the stability cable is 25kN and 55kN respectively, the first frequencies of the new flexible photovoltaic system are 1.46Hz and 1.76Hz respectively, and the simulation results are consistent with the test results. Figure. 2a and figure. 2b show the statistical error analysis of the finite element simulation and test results under tensile process and different loading conditions, respectively. The error distribution conforms to the normal distribution. The mean error and standard deviation under tensile process are 1.44% and 3.46%. Under different loading conditions, the mean error is 0.67% and the standard deviation is 4.4%. This means that the finite element simulation can simulate the tension and stress state of the system accurately, and the tension scheme proposed in this paper can control the tension of the cable precisely.

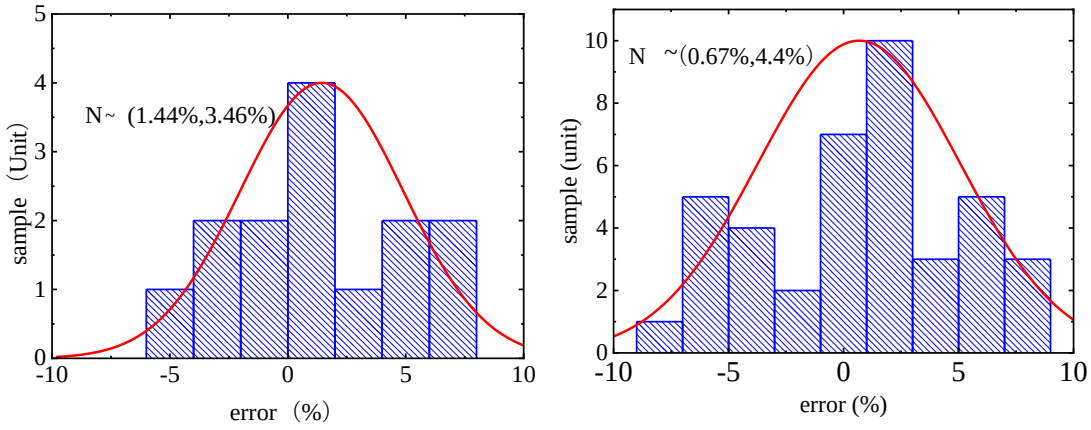

Figure. 2. Error statistics of cable force: (a) cable tension complete, (b) different loading conditions.

2.3 Dynamic characteristic

The dynamic characteristics of the cable-truss flexible photovoltaic support system and the double-layer cable-supported flexible photovoltaic support system are compared. The component cable of the cable-support flexible photovoltaic support system is horizontal state, and the stability cable deflection-span ratio is 1/15 (figure. 3). Other design parameters are consistent with those of the new flexible photovoltaic support system. Figure. 4 shows the vibration mode of the two structural systems, and Table 2 shows the calculation results of natural vibration frequencies. It can be found that the first mode of the cable-supported flexible photovoltaic support system is vertically symmetric in the span, the second mode is the vertical antisymmetric half-wave vibration, the third mode is the mid-span torsional vibration, and the first three frequencies are 1.587Hz, 1.751Hz and 2.494Hz respectively. The first model

of the three-dimensional cable-truss flexible photovoltaic support system is vertical antisymmetric half-wave vibration, the second mode is vertical symmetric vibration of 1/3 wave, the third mode is mid-span torsional vibration, and the first three frequencies are 1.762Hz, 2.481Hz and 3.333Hz, respectively. The results show that the frequencies of the first three modes of the three-dimensional cable-truss flexible photovoltaic support system increase by 11.0%, 37.6%, and 28.7%, respectively, and the modal changes are obvious and the structural stiffness is greater. This can play a certain role in reducing the wind-induced vibration of the flexible photovoltaic support system.

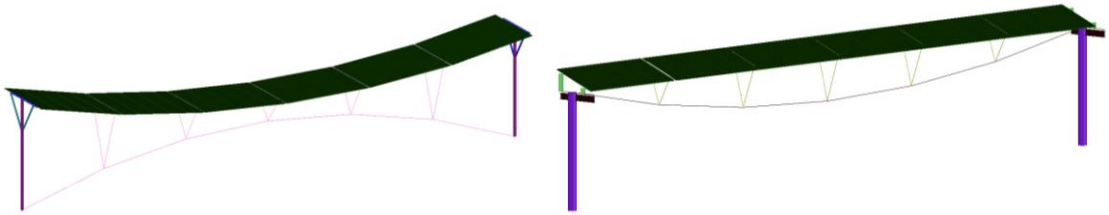

(a) (b)

Figure. 3. Finite element model: (a) the cable-truss flexible photovoltaic support system; (b) the cable-supported photovoltaic module system.

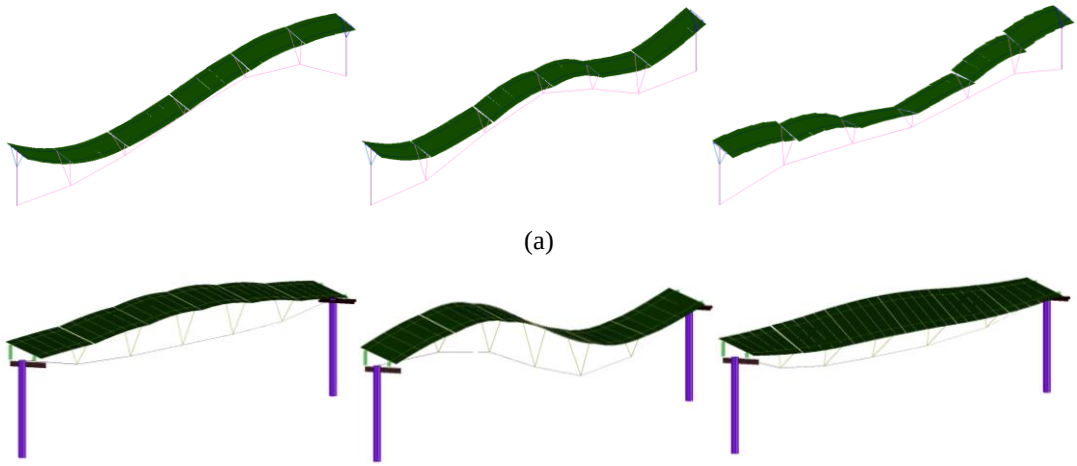

(a)

(b)

Fig. 4. The first three vibration modes: (a) cable-truss flexible photovoltaic support system: 1st, 2nd, 3rd, (b) cable-supported photovoltaic module system: 1st, 2nd, 3rd.

Table 2: Comparison of vibration frequency of two kinds of flexible photovoltaic support structures.

Name	Initial tension（kN）		Frequency (Hz)		
	Cable 1(cable 2)	Cable 3	1st	2ed	3rd
Cable-support	45	55	1.587	1.751	2.494
Cable-truss	45	55	1.762	2.481	3.333

2.4 Stiffness comparison

To further compare the mechanical properties of the new flexible support system with the cable-supported flexible photovoltaic support system, the nonlinear mechanical properties of the two systems were analyzed. In addition to the dead load of the flexible photovoltaic support system, wind load is the main load on the flexible photovoltaic support system. Considering wind pressure and wind suction, the wind load was increased from 0kN/m^2 to 2kN/m^2 (corresponding to an average wind speed of 56.6m/s). Figure 5 shows the two cases of wind pressure (case 1) and wind suction (case 2) respectively. The load-displacement curves of two kinds of flexible photovoltaic support systems in case 1 and case 2 are compared. The horizontal deformation is calculated according to Eq. (1), the vertical deformation is

calculated according to Eq. (2), and the torsional deformation is calculated according to Eq. (3). Since the deformation of the flexible photovoltaic support system along the span is small, the variation law of the span direction displacement is not considered. The horizontal stiffness, vertical stiffness, and torsional stiffness of the system are calculated according to Eq. (4) to Eq. (6).

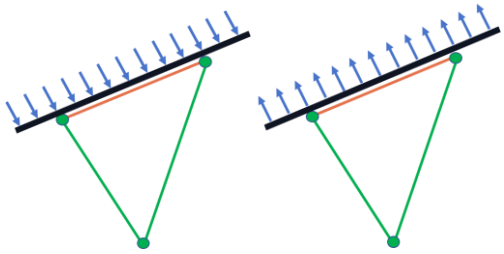

(a) (b)

Figure. 5. Loading condition. (a) Wind pressure, (b) Wind suction.

$$H = \frac{h_1 + h_2}{2} \tag{1}$$

$$Z = \frac{z_1 + z_2}{2} \tag{2}$$

$$\theta = \arctan\left(\frac{z_2 - z_1}{D}\right) \tag{3}$$

Where h_1 and h_2 are the Y-axis displacements of the Cable 1 and Cable 2 in 1/2 span, z_1 and z_2 are the Z-axis displacements of the Cable 1 and Cable 2 in 1/2 span, D is the distance of Cable 1 and Cable 2, respectively.

$$K_h = \frac{F}{H} \tag{4}$$

$$K_v = \frac{F}{Z} \tag{5}$$

$$K_t = \frac{F}{\theta} \tag{6}$$

Where F is the uniform pressure on the surface of the PV module, and the unit is kN/m^2.

Figure. 6 shows the load-displacement change curves of the two systems under wind suction. It can be found in the figure. 6a and figure. 6b that the horizontal stiffness of the new flexible photovoltaic support system is reduced from the initial 12.22kN/m^3 to 5.23kN/m^3, and then gradually increased to 7.76kN/m^3, while the stiffness of the cable-support flexible photovoltaic system is gradually increased from 7.54kN/m^3 to 18.42kN/m^3. The vertical stiffness of the new flexible photovoltaic support system gradually decreased from the initial 15.02kN/m^3 to 3.52kN/m^3, and the stiffness of the cable-support flexible photovoltaic system gradually increased from the initial 2.92kN/m^3 to 6.84kN/m^3. Under the action of wind suction, when the wind load value is less than 0.44kN/m^2, the horizontal displacement of the new flexible photovoltaic support system is less than that of the cable-support flexible photovoltaic system. When the wind load is less than 1.54kN/m^2, the vertical displacement of the new flexible photovoltaic support system is less than that of the cable-supported flexible photovoltaic system. Under the action of wind suction, when the wind load is less than 0.44kN/m^2 and 1.54kN/m^2, the three-dimensional cable-truss flexible photovoltaic support system has better horizontal and vertical stiffness.

Figure. 6c, 6d, and 6e show that the stiffness in the horizontal direction, vertical direction and torsional direction of the two systems under wind pressure increases with the increase of wind load. Under wind pressure, the horizontal stiffness of the new flexible photovoltaic support system is maintained at 37.74kN/m^3, and the stiffness of the cable-support flexible photovoltaic system is gradually increased from the initial 7.75kN/m^3 to 19.36kN/m^3. The vertical stiffness of the new flexible photovoltaic support

system was maintained at 37.60kN/m^3, and the stiffness of the cable-support flexible photovoltaic system gradually increased from the initial 2.92kN/m^3 to 6.63kN/m^3. The torsion stiffness of the new flexible photovoltaic support system was maintained at 118.89kN/m^2·rad, and the stiffness of the cable-support flexible photovoltaic system gradually increased from the initial 45.40kN/m^2·rad to 97.49kN/m^2·rad. The structural stiffness of the new flexible photovoltaic support system under wind pressure is always much higher than that of cable-support flexible photovoltaic support.

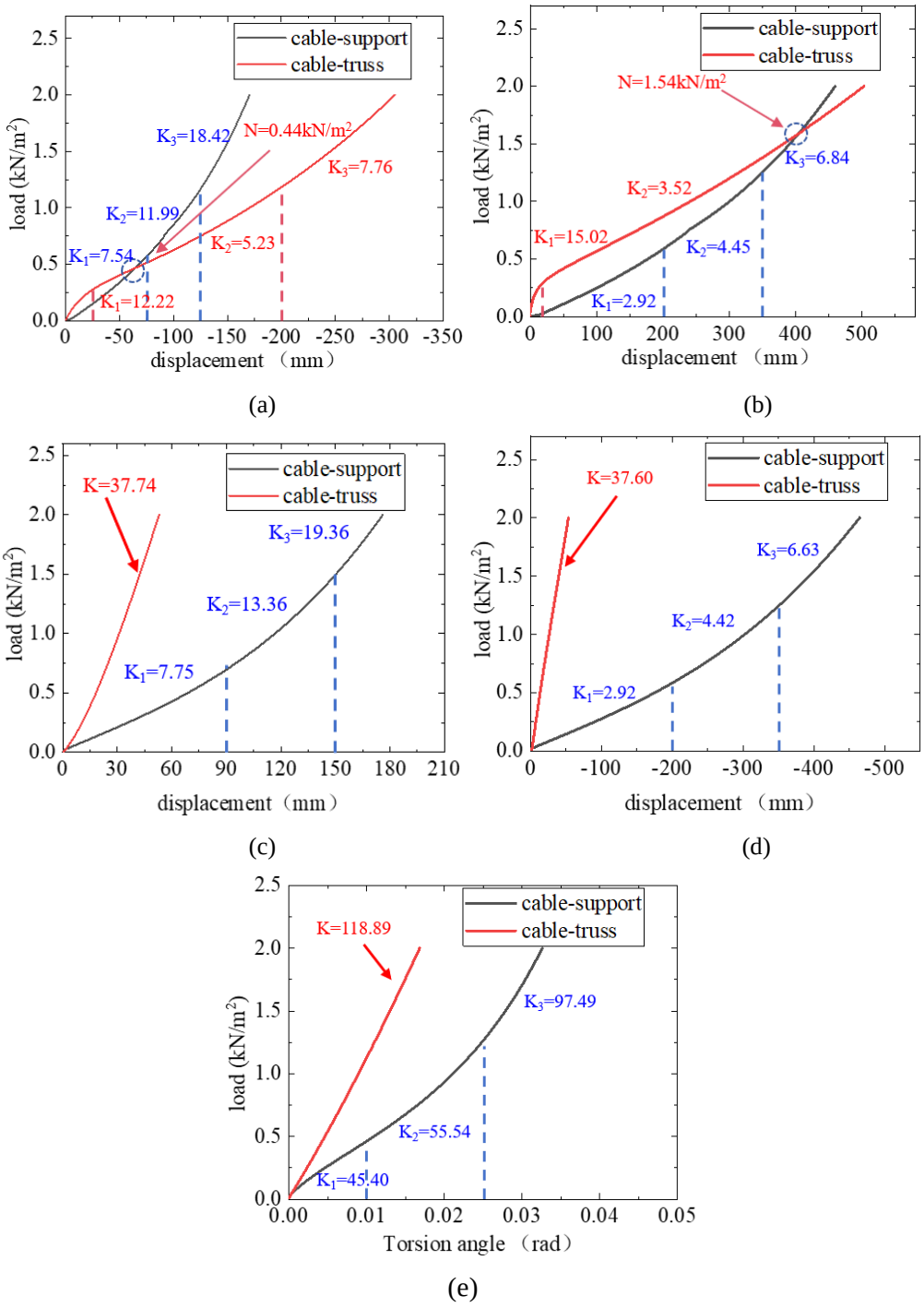

Figure. 6. Load-deformation curve. (a) horizontal deformation under wind pressure, (b) vertical deformation under wind pressure, (c) horizontal deformation under wind suction, (d) Vertical deformation under wind suction, (e) torsion deformation under wind pressure.

3. Parametric analysis

3.1. Deflection-span ratio and rise-span ratio

The influence of the component cable deflection-span ratio (1/15, 1/20, 1/25) and the stability cable rise-span ratio (1/15, 1/20, 1/25) on system design parameters is analyzed. It can be found that the decrease of the component cable deflection-span ratio or the stability cable rise-span ratio will lead to the increase of the initial tension of the component cables and the increase of the natural vibration frequency (figure. 7a, figure. 7b). When the component cable deflection-span ratio is reduced by 1/5, the initial tension of the component cable needs to be increased by 5kN. For every 1/5 reduction in he stability cable rise-span ratio, the initial tension of stability cable needs to increase by 10kN, and the reduction of the rise-span ratio of stability cable has a greater impact on the initial tension of the stability cable (figure. 7b). The reduction of the component cable deflection-span ratio has little effect on the initial tension of stability cable, and the reduction of t the stability cable rise-span ratio will lead to a significant increase on the initial tension of stability cable (figure. 7c). When the stability cable rise-span ratio is reduced by 1/5, the initial tension of stability cable needs to be increased by about 20kN.

3.2. Span and spacing

In addition, the influence of different spans of 25m, 35m, 45m, 55m, and 65m on the initial tension of component cable and stability cable is also analyzed. The results show that when the span is 25 meters, the initial tension of component cable is only 55kN. However, when the span reaches 65 m, the initial tension of the component cable is increased to 80kN. The initial tension of the stability cable can be maintained at 70kN when the span is increased from 25m to 65m (figure. 7d). This illustrates that the increase of the span of the new system has a greater impact on the initial tension of component cable, but has almost no impact on the initial tension of stability cable. The increase of span will have a great influence on the change of vibration frequency, and will significantly reduce the vibration frequency. The span of the system is increased from 25m to 65m, and the vibration frequency is reduced from 0.96 to 0.47, reducing by more than 50% (figure. 7e).

The influence of different cable spacing 4m, 5m, 6m, 7m, and 8m on the vibration frequency of the system is analyzed. The results show that the stiffness of the system decreases with the increase of cable spacing. The increase in cable spacing from 4m to 7m resulted in a decrease in vibration frequency of approximately 12.8% (figure 7f).

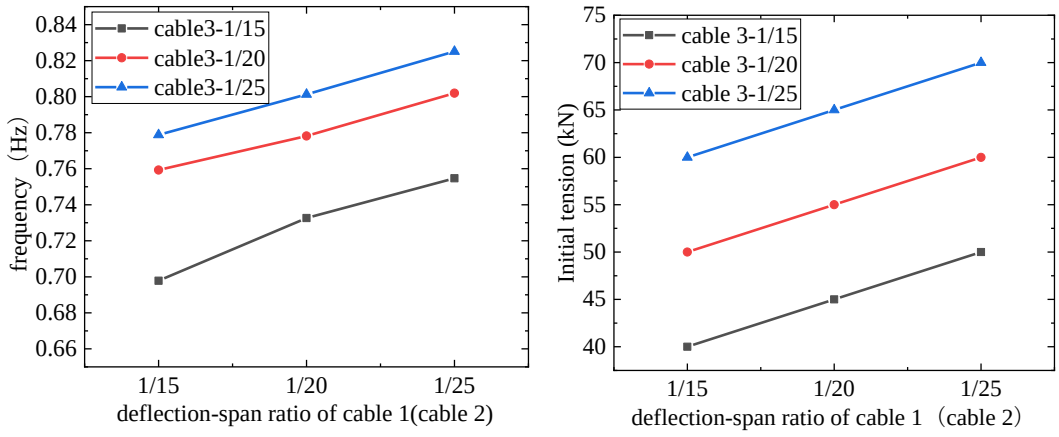

(a) (b)

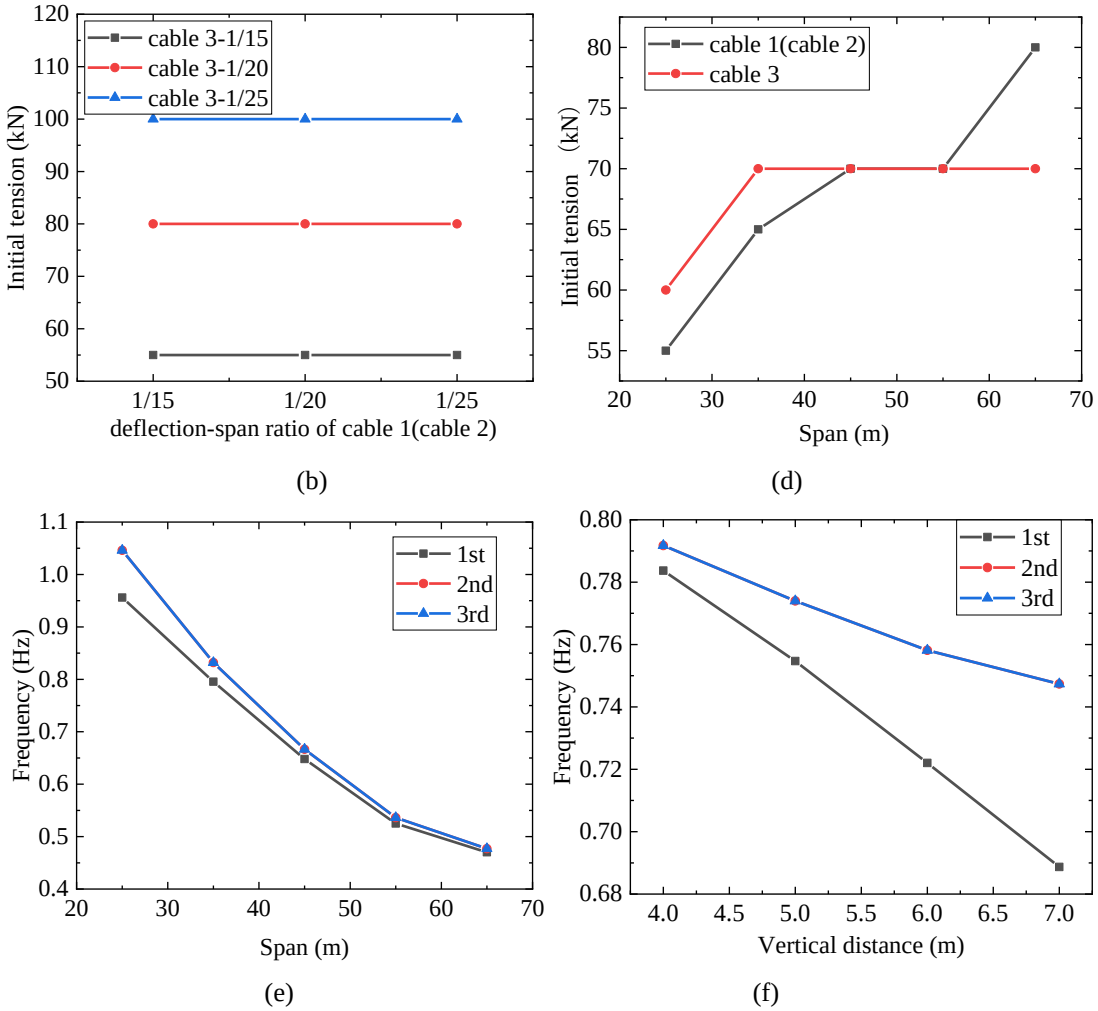

Fig. 7. The results of parametric analysis: (a) The influence of the ratio of deflection-span of the component cable (rise-span ratio of the stability cable) on frequency, (b) The influence of the ratio of deflection-span of the component cable (rise-span ratio of the stability cable) on the component cable initial tension, (c) The influence of the ratio of deflection-span of the component cable (rise-span ratio of the stability cable) on the stability cable initial tension, (d) The influence of span on the component cable initial tension, (e) The influence of span on frequency, (f) The influence of the distance between cables on the frequency.

3.3. Initial tension

It can be found that the increase of the initial tension of component cable and stability cable can increase the vibration frequency (figures. 8a and 8b). The increase of initial tension of the component cable has no obvious effect on the increase of vibration frequency. The initial tension is increased from 30kN to 70kN, and vibration frequency is increased from 1.170Hz to 1.195Hz, and the vibration frequency of is only increased by 2.1% (figure. 8a). However, the initial tension of the stability cable is increased from 30kN to 70kN, the vibration frequency is increased from 1.13Hz to 1.31Hz, and the vibration frequency is increased by 16% (figure. 8b).

3.4. PV module tilt angle

The tilt angle of PV modules will lead to the reduction of vibration frequency, but the impact on that is not large. The tilt angle of PV modules is increased from 5° to 30°, and the vibration frequency is only reduced by 4% (figure. 8c).

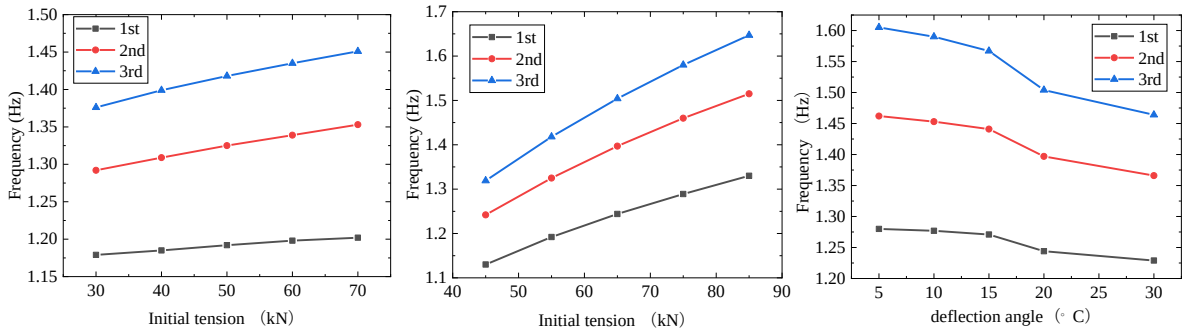

(a) (b) (c)

Figure. 8. The results of parametric analysis of dynamic characteristics: (a) The influence of the initial tension of component cable on the frequency, (b) The effect of the initial tension of stability cable on the frequency, (c) The influence of the tilt angle on the frequency.

Through the above analysis, it can be concluded that reducing the deflection-span ratio of component cable or the rise-span ratio of stability cable will lead to an increase in system stiffness, and the initial tension of the component cable needs to increase in response. The reduction of the deflection-span ratio of component cable has little effect on the initial tension of the stability cable, but the reduction of the rise-span ratio of stability cable will lead to an obvious increase in the initial tension of the stability cable. The initial tension of the stability cable, the distance between the component cable and the stability cable, and the span have obvious effects on system stiffness. The initial tension of the component cable and PV module tilt angle has little influence on system stiffness.

4. Conclusion

In this paper, the advantages of mechanical properties of a new three-dimensional cable-truss flexible photovoltaic support system are demonstrated by nonlinear finite element analysis. The accuracy of the finite element simulation is verified by the 35-meter span prototype test. Meanwhile, the influence of some design parameters on the initial tension and vibration frequency is revealed through parameter analysis. The main conclusions are as follows.

(1) Compared with the 35-meter span cable-supported flexible photovoltaic system, the three-dimensional cable-truss flexible photovoltaic support system has obvious structural modal changes, the first three vibration frequencies increased by 11.0%, 37.6%, 28.7%, and the overall stiffness has been greatly improved. The accuracy of finite element simulation results is verified by a full-scale test.

(2) The reduction in the deflection-span ratio or the rise-span ratio causes the component cable and the stability cable to provide more initial tension. The stability cable initial tension, span, and cable spacing are the main factors affecting the stiffness of the system. The initial tension of the component cable and the tilt angle of the PV module have little effect on the stiffness of the system.

Acknowledgments

This research is financially supported by the National Natural Science Foundations of China (No. 52378144, 52178134) and the Natural Science Foundation of Heilongjiang Province of China (No. LH2021E076).

References

[1] Bartholet, R.; A. Büchel; Baumgartner, F. Solar Ski Lift PV Carport and Other Solar Wings Cable Based Solutions. . 2012, doi:10.4229/27THEUPVSEC2012-5BV.1.60.

[2] Baumgartner, F.; A. Büchel; Carigiet, F.; Baumann, T.; Epp, R.; Wirtz, A.; A. Hügeli; Graf, U. “‘Urban Plant’” Light-Weight Solar System for Parking and Other Urban Double Use Applications. . 2013, doi:10.21256/ZHAW-4896.

[3] A. Büchel; Bartholet, R. SOLAR WINGS A NEW LIGHTWEIGHT PV TRACKING SYSTEM. . 2008, doi:10.4229/23RDEUPVSEC2008-4DO.9.5.

[4] Bartholet, R.; A. Büchel; Baumgartner, F. Experiences with Cable-Based Solar Wings Tracking System and Progress towards Two-Axis Large Scale Solar System. . 2009, doi:10.4229/24THEUPVSEC2009-4CO.8.6.

[5] Bartholet, R.; A. Büchel; Baumgartner, F. Cable-Based Solar Wings Tracking System: Two-Axis System and Progress of One-Axis System. . 2010, doi:10.4229/25THEUPVSEC2010-4BV.1.34.

[6] Tamura, Y.; Kim, Y.C.; Yoshida, A.; Itoh, T. Wind-Induced Vibration Experiment on Solar Wing. MATEC Web Conf. 2015, 24, 04006, doi:10.1051/matecconf/20152404006.

[7] Kim, Y.; Tamura, Y.; Yoshida, A.; Ito, T.; Shan, W.; Yang, Q. Experimental Investigation of Aerodynamic Vibrations of Solar Wing System. Adv. Struct. Eng. 2018, 21, 2217–2226, doi:10.1177/1369433218770799.

[8] Wang Zeguo, Zhao Feifei, Ji Chunming, et al. Wind-induced response analysis of Large-span flexible photovoltaic scaffolds [J]. Proceedings of Civil Engineering Symposium on New Materials, New Technologies and Engineering Applications (Vol. 2), 2019: 757-760+785, doi:10.26914/c.cnkihy.2019.046261.

[9] Wang Zeguo, Zhao Feifei, Ji Chunming, et al. Wind-induced vibration analysis of multi-row and multi-span flexible photovoltaic scaffolds [J]. Engineering Journal of Wuhan University, 2021(S2): 75–79.

[10] Ma Wenyong, Chai Xiaobing, Ma Chengcheng. Experimental study on influence factors of wind load on flexible supported photovoltaic modules [J]. Acta Solar Energy Sinica, 2021(11): 10-18, doi:10.19912/j.0254-0096.tynxb.2019-1184.

[11] He, X.-H.; Ding, H.; Jing, H.-Q.; Wu, X.-P.; Weng, X.-J. Mechanical Characteristics of a New Type of Cable-Supported Photovoltaic Module System. Solar Energy 2021, 226, 408–420, doi:10.1016/j.solener.2021.08.065.

[12] He, X.; Cai, C.; Wang, Z.; Jing, H.; Qin, C. Experimental Verification of the Effectiveness of Elastic Cross-Ties in Suppressing Wake-Induced Vibrations of Staggered Stay Cables. Eng. Struct. 2018, 167, 151–165, doi:10.1016/j.engstruct.2018.04.033.

[13] Ding, H.; He, X.; Jing, H.; Wu, X.; Weng, X. Design Method of Primary Structures of a Cost-Effective Cable-Supported Photovoltaic System. Appl. Sci. 2023, 13, 2968, doi:10.3390/app13052968.

[14] Liu, J.; Li, S.; Luo, J.; Chen, Z. Experimental Study on Critical Wind Velocity of a 33-Meter-Span Flexible Photovoltaic Support Structure and Its Mitigation. J. Wind. Eng. Ind. Aerodyn. 2023, 236, 105355, doi:10.1016/j.jweia.2023.105355.

[15] Xu Zhihong. Numerical Analysis of Wind Vibration Response of Fish-belly Photovoltaic Cable Truss [J]. Proceedings of 2020 Industrial Building Academic Exchange (Volume 2), 2020:363-365 +257, doi:10.26914/c.cnkihy.2020.024214.

[16] Zhou Jie, Du Jine, Xu Jialuo, et al. Design and analysis of prestressed cables of photovoltaic flexible support under mountainous terrain [J]. Proceedings of 2020 Industrial Building Academic Exchange Conference (Volume 2), 2020:375-379, doi:10.26914/c.cnkihy.2020.024217.

[17] Xu Haiwei, Lou Wei, Li Tianhao, et al. Experimental study on size coefficient of Large-span PV scaffold structure [J]. Proceedings of 2021 Industrial Building Academic Exchange, 2021: 340-344, doi:10.26914/c.cnkihy.2021.048865.

[18] He, X.-H.; Ding, H.; Jing, H.-Q.; Zhang, F.; Wu, X.-P.; Weng, X.-J. Wind-Induced Vibration and Its Suppression of Photovoltaic Modules Supported by Suspension Cables. J. Wind. Eng. Ind. Aerodyn. 2020, 206, 104275, doi:10.1016/j.jweia.2020.104275.

[19] Chen, F.; Zhu, Y.; Wang, W.; Shu, Z.; Li, Y. A Review on Aerodynamic Characteristics and Wind-Induced Response of Flexible Support Photovoltaic System. Atmosphere. (Basel). 2023, 14, 731, doi:10.3390/atmos14040731.